

Kinetics of the reversible inclusion of flavopereirine in cucurbit[7]uril

Zsombor Miskolczy,^a László Biczók^{*a}, and István Jablonkai^b

^aInstitute of Materials and Environmental Chemistry, Research Centre for Natural Sciences, Hungarian Academy of Sciences, P.O. Box 286, 1519 Budapest, Hungary

^bInstitute of Organic Chemistry, Research Centre for Natural Sciences, Hungarian Academy of Sciences, P.O. Box 286, 1519 Budapest, Hungary

* Corresponding author. E-mail: biczok.laszlo@tk.mta.hu

ABSTRACT

The temperature dependence of the kinetics of flavopereirine inclusion in cucurbit[7]uril (CB7) was studied by stopped-flow method in water. The substantial blue-shift of the emission band and the ~4-fold fluorescence quantum yield enhancement upon host-guest binding permitted the monitoring of the formation and dissociation of the flavopereirine–CB7 1:1 complex in real time. The competitive binding of 1-adamantylammonium cation with extremely high affinity was exploited to selectively and very accurately determine the kinetic parameters of the flavopereirine exit from CB7 cavity. The rate constants of the ingress into and the egress from CB7 were found to be $9.0 \times 10^7 \text{ M}^{-1}\text{s}^{-1}$ and 1.6 s^{-1} at 298 K, respectively. Both processes had substantial activation enthalpy implying that a steric barrier had to be overcome in the course of the reversible encapsulation. The $31 \pm 2 \text{ kJ mol}^{-1}$ activation enthalpy of the entry into CB7 was comparable to the $37 \pm 2 \text{ kJ mol}^{-1}$ enthalpy change upon the complex dissociation.

INTRODUCTION

Cucurbit[*n*]urils (CBn), the family of macrocyclic molecular containers composed of *n* glycoluril units bound by a pair of methylene groups, have great potential in the delivery and controlled release of drugs.¹⁻⁶ These water-soluble cavitands are nontoxic^{7,8} and can encapsulate molecules of pharmacological interest improving their solubility and bioavailability. They can serve as nanocapsules to promote the transportation of drugs into cells. Partial embedment in CBn may provide a formulation method for clinical application of platinum-based anti-cancer agents.^{9,10} Inclusion in cucurbit[7]uril (CB7) significantly enhanced the thermal stability of ranitidine, a drug used for the treatment of excess stomach acid,¹¹ and resulted in strongly bound complexes possessing pH-responsive behaviour for local anaesthetics.¹² The confinement of the proton-pump inhibitor lansoprazole and omeprazole drugs in CB7 catalysed the transition into their physiologically active cyclic sulfonamide form and impeded the decomposition and dimerization.¹³

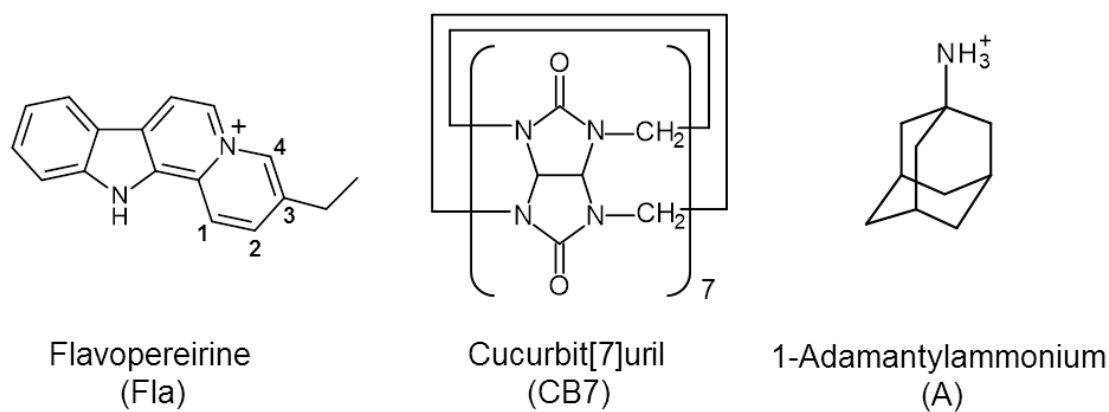
Due to the pharmaceutical importance of natural alkaloids, their self-assembly with CBn has received particular attention. The effect of inclusion complex formation on the solubility and anticancer activity of camptothecin was revealed.¹⁴ Host-guest association with CB7 brought about only 0.7 pK unit rise in the basicity of norharmane¹⁵ but substantially inhibited the nucleophilic addition of hydroxide anions to sanguinarine cation and hindered the photooxidation.¹⁶ Berberine binding in CB7 resulted in about 500-fold fluorescence quantum yield growth,¹⁷ which was exploited to monitor the passage of biologically important compounds into liposomes and through bacterial transmembrane protein.¹⁸ The intense fluorescence of CB7 complexes was used in the quantitative analysis of alkaloids in biological fluids.^{19,20}

Despite the pivotal importance of the dissociation rate of the active ingredients in the design of pharmaceutical formulations, knowledge of the kinetics of the reversible host-guest

complex formation of CB7 is scarce²¹⁻²³ and only a single study has been published on the activation parameters of entry into and exit from the nonpolar CB7 cavity.²⁴ Large activation enthalpy was found for berberine ingress implying that considerable steric distortion occurred when the guest passed through the tight carbonyl-laced opening of CB7. Both inclusion and dissociation were much more rapid for the less spacious 6-methoxy-1-methylquinolinium²⁵ and (*R*)-(+)-2-naphthyl-1-ethylammonium²⁶ cations indicating the rate determining role of the molecular dimensions. Kaifer and co-workers observed enormous solvent effect on the kinetics of the pseudorotaxane-type complex formation of dumbbell-shaped guests whose ingress into CB7 cavity was significantly faster in water than in DMSO.²⁷ The quick 1:1 binding of the flavylium cation form of an anthocyanin in CB7 was exploited to stabilize the dye colour since decomposition via hydration could not compete with the formation of the inclusion complex in water.²⁸ Bohne and Thomas demonstrated with systematic studies that the CB7 complex of 2-aminoanthracenium cation can form not only by direct inclusion but also via the initial encapsulation of 2-aminoanthracene followed by protonation.²⁹ The substantial pK_a increase upon host-guest binding was found to arise from the slower deprotonation in the cavity of CB7 than in water.

The present work focuses on the kinetics of the reversible confinement of flavopereirine (3-ethyl-12*H*-indolo[2,3-*a*]-quinolizinium perchlorate) (Fla) in CB7. This biologically important alkaloid, originally isolated from the bark of an Amazonian tree family known as pao pereira in Brasil,³⁰ may possess antiparasitic and cytotoxic activity.^{31,32} The fluorescence characteristics of Fla are solvent-sensitive and significantly change upon interaction with nucleotides, DNA and chondroitin-6-sulfate.³³ Therefore, inclusion in CB7 is expected to modify the fluorescent behaviour allowing the monitoring of the dynamics of complex formation in real time. Because host-guest complexes are in dynamic equilibrium with their components, direct measurements of

association or dissociation contain information on the rate constants of ingress (k_+) and egress (k_-) alike. To enhance the accuracy of the obtained kinetic parameters, we intend to apply a simple straightforward fluorescent method for the separate determination of k_- . Our main objectives are to reveal how the variation of temperature influences the kinetics of the elementary reaction steps and to get information of the properties of the transition states. The formulas of the employed compounds are displayed in Scheme 1.



Scheme 1 Chemical structure of the used compounds

EXPERIMENTAL

Flavopereirine perchlorate (Fla) (ChromaDex) and 1-adamantylamine (Aldrich) were used without further purification. The latter compound is fully protonated at neutral pH since its conjugated acid has a pK_a value³⁴ of 10.55. High-purity CB7 was kindly provided by Dr. Anthony I. Day (University of New South Wales, Canberra, Australia). Experiments were carried out in double distilled water. Fla concentrations were determined spectrophotometrically using molar absorption coefficient $15070 \text{ M}^{-1}\text{cm}^{-1}$ at 384 nm in water. The UV-visible absorption spectra were obtained on an Agilent Technologies Cary60 spectrophotometer. Corrected fluorescence spectra were recorded on a Jobin-Yvon Fluoromax-P photoncounting

spectrofluorometer. Stopped-flow measurements were performed with the same instrument using an Applied Photophysics RX2000 rapid mixing accessory and a pneumatic drive. The temperature of the samples was controlled with a Julabo F25-ED thermostat. Fluorescence decays were measured with time-correlated single-photon counting technique using the previously described instrument.³⁵ The results of spectrophotometric and fluorescence titrations as well as stopped-flow measurements were analysed with homemade programs written in MATLAB 7.9. Semiempirical calculations with RM1 method were carried out with HyperChem 8.0 program.

NMR spectra were acquired on a Varian 500 Inova spectrometer, running at 500 MHz for ¹H. Chemical shifts (δ) are reported in ppm relative to residual solvent signals (CHCl₃, 7.26 ppm for ¹H NMR). The following abbreviations are used to indicate the multiplicity in ¹H NMR spectra: s, singlet; d, doublet; t, triplet; m, multiplet; bs, broad signal. Assignments for Fla and Fla–CB7 complex are as follows. Fla (D₂O, ppm): 1.42 (t, 3H, CH₃), 2.94 (q, 2H, CH₂), 7.36 (m, 1H, arH), 7.62 (bs, 2H, arH), 8.08 (d, 1H, arH), 8.12 (d, 1H, arH), 8.29 (d, 1H, arH), 8.31 (d, 1H, arH), 8.48 (d, 1H, arH), 8.72 (s, 1H, arH, H-4). Fla–CB7 (D₂O, ppm): 0.86 (bs, 3H, CH₃), 2.22 (bs, 2H, CH₂), 4.25 (d, 14H, CH₂, CB7), 5.52 (s, 14H, CH, CB7), 5.73 (bs, 14H, CH₂, CB7), 7.24 (bs, 1H, arH), 7.52 (bs, 1H, arH), 7.78 (bs, 1H, arH), 7.79 (bs, 3H, arH), 8.41 (bs, 1H, arH), 8.70 (bs, 1H, arH), 8.85 (bs, 1H, arH).

RESULTS

Effect of CB7 on the absorption and fluorescence properties

Figure 1A presents the alteration of the absorption spectrum of 10.7 μ M Fla upon addition of 26.1 μ M CB7 in water. The lowest energy absorption maximum exhibits hypochromicity and

about 4 nm red-shift due to inclusion complex formation. The confinement of Fla in the nonpolar cavity of CB7 leads to a substantial fluorescence intensity enhancement accompanied by a 21 nm hypsochromic displacement of the spectrum maximum (Figure 1B). After an initial linear rise, the fluorescence intensity at 440 nm levels off at equimolar [CB7]/[Fla] concentration ratio, corroborating the 1:1 stoichiometry of binding.

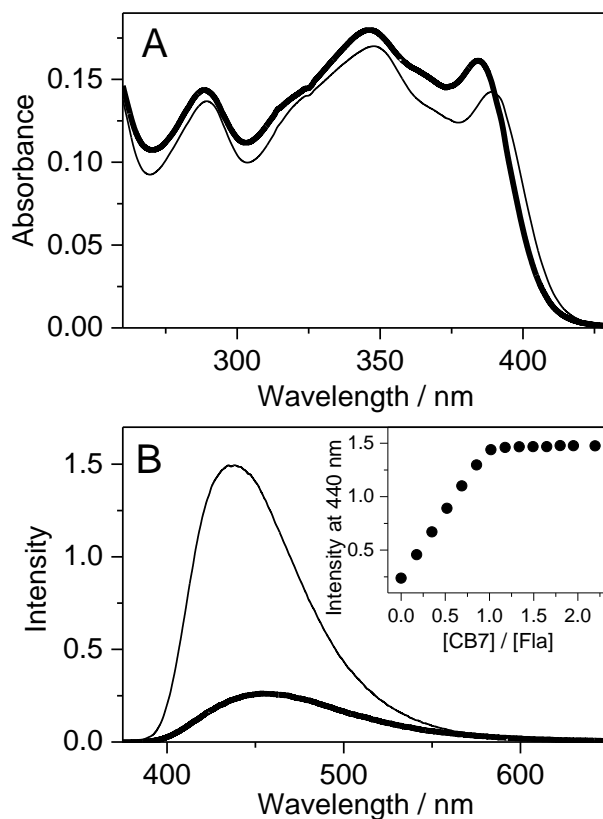


Figure 1 Absorption (A) and fluorescence (B) spectra of 10.7 μM Fla in water (thick line) and in 26.1 μM CB7 aqueous solution (thin line) at 296 K (optical path 1 cm, excitation at 390 nm). Inset: fluorescence intensity at 440 nm as a function of [CB7]/[Fla] concentration ratio.

The photophysical parameters of the free and CB7-bound Fla are summarized in Table 1. Figure S1 in Supplementary Information illustrates why the inclusion in the apolar CB7 cavity leads to red-shift in the absorption whereas blue-shift in the fluorescence spectra. The energy of the

Table 1 Variation of absorption (λ_a) and fluorescence (λ_f) maxima, energy of the lowest singlet-excited state ($E(S_1)$), fluorescence quantum yield (Φ_f), fluorescence lifetime (τ_f), rate constant of fluorescence (k_f) and nonradiative deactivation (k_{nr}) for 10.7 μ M flavopereirine in water and 26.1 μ M CB7 aqueous solution.

solvent	λ_a /nm	λ_f /nm	$E(S_1)$ /kJ mol ⁻¹	Φ_f	τ_f /ns	k_f /10 ⁷ s ⁻¹	k_{nr} /10 ⁷ s ⁻¹
H ₂ O	385	459	291.9	0.11	5.0	2.2	17.8
26.1 μ M CB7 H ₂ O	389	438	294.7	0.43	12.8	3.4	4.5

lowest singlet-excited state ($E(S_1)$) was calculated from the location of the intersection of the normalised absorption and fluorescence spectra plotted at wavenumber scale. Remarkable increases in the quantum yield (Φ_f) and lifetime (τ_f) of fluorescence are observed upon encapsulation in CB7. The rate constants for radiative (k_f) and nonradiative (k_{nr}) deactivations from the singlet-excited state are calculated using the expressions $k_f = \Phi_f/\tau_f$ and $k_{nr} = (1-\Phi_f)/\tau_f$. The dominant change appears in the latter quantity, whereas k_f grows only about 55% upon host-guest complexation. We have demonstrated that the photophysical characteristics of Fla are solvent dependent.³⁶ The remarkable deuterium isotope effect on τ_f suggested that hydrogen bonding of the singlet-excited Fla offers an effective pathway for dissipation of excitation energy. The partial inclusion in the CB7 core provides a nonpolar, extremely nonpolarizable microenvironment for the guest³⁷ and diminishes its interaction with water decelerating thereby radiationless deactivation from the singlet-excited state. The increase of k_f in CB7 can be rationalized in terms of the Strickler-Berg equation³⁸

$$k_f = 2.88 \times 10^{-9} n^2 (\bar{\nu}^{-3})_{av}^{-1} \int \epsilon d \ln \bar{\nu} \quad (1)$$

where n denotes the refractive index of the microenvironment, $(\bar{\nu}^{-3})_{av}^{-1}$ is an average over the fluorescence spectrum and the integral of molar absorption coefficients (ϵ) extends over the first absorption band. This relationship predicts that k_f grows approximately as the cube of the emission energy. Hence, the blue-shift of the fluorescence spectrum due to the embedment in CB7 results in larger k_f . On the basis of the comparison of the photophysical properties in various solvents³³ and CB7, we conclude that Fla senses somewhat less polar surroundings in CB7 than in acetonitrile.

Structure of the inclusion complex

The energy-minimized structure of Fla–CB7 complex was calculated by RM1 semiempirical method using HyperChem 8.0 program. The result shows (Figure 2) that the ethyl substituent of Fla is fully confined in the hydrophobic core of CB7, whereas the quinolizinium moiety is only

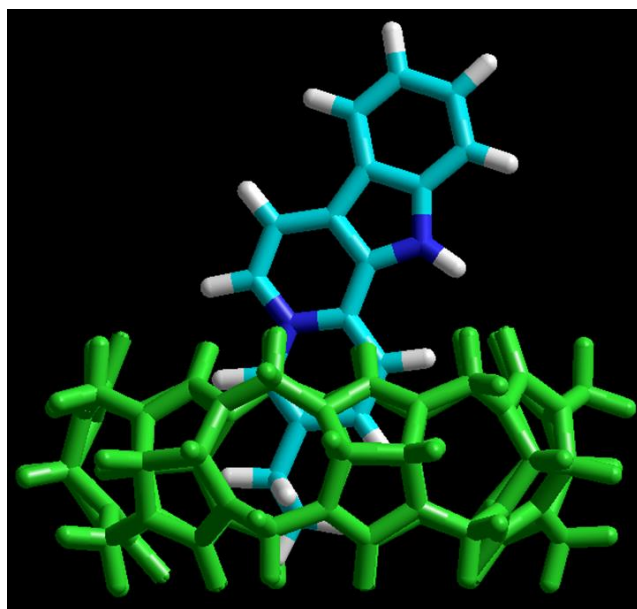


Figure 2 Energy-minimized structure of Fla–CB7 inclusion complex calculated by RM1 method

Color codes: CB7, green; nitrogen, blue; carbon, light blue; hydrogen, white

partially encapsulated and its nitrogen is located in the vicinity of the carbonyl-rimmed portal of the host. The indole segment of Fla is not embedded. It protrudes into the aqueous phase. The charge of Fla is delocalized and mainly appears as low electron density on the peripheral hydrogens of the ring system. The carbon atom fusing the aromatic rings of quinolizinium also has a partial positive charge, which is located in the neighbourhood of the oxygen atoms at the entrance of CB7 cavity.

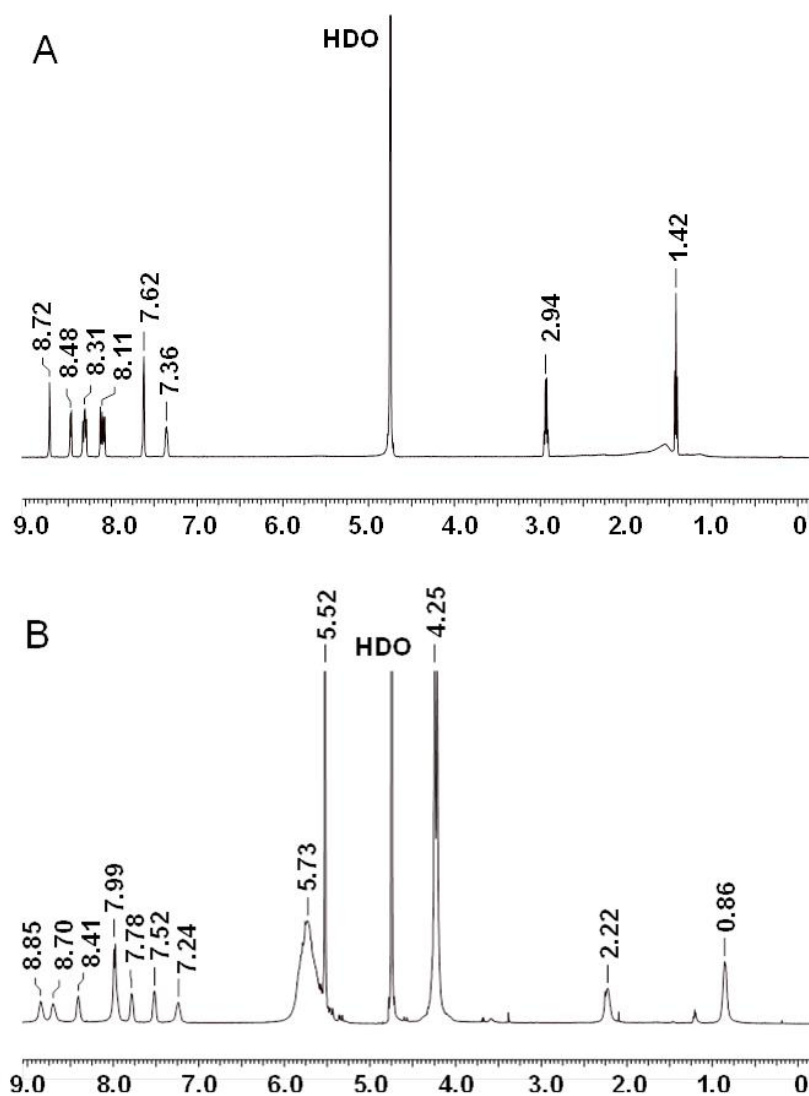


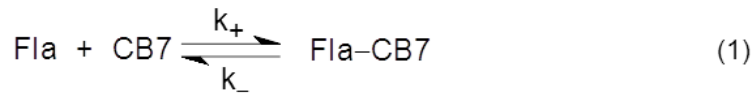
Figure 3 ^1H NMR spectra of Fla (A) and Fla-CB7 complex (B) recorded in D_2O

¹H NMR spectra of Fla and Fla–CB7 recorded in D₂O (Figure 3) corroborated the calculated structure of the inclusion complex. The addition of 1 equivalent of CB7 yielded remarkable spectral changes in the Fla spectrum (Figure 3B). The signals of the ethyl group broadened and exhibited 0.6-0.7 ppm upfield shift indicating, in accordance with the results of calculations, that the ethyl group is fully embedded in the interior of CB7. Both downfield and upfield shifts of the resonances of the aromatic protons were found. Because of the poor solubility of both host and guest molecules in D₂O, no exact assignments of the aromatic protons were made but probably the singlet peak of the methine proton (H-4, δ 8.72 ppm) adjacent to the nitrogen atom of the quinolizinium moiety as well as the H-1 and H-2 proton signals of this heterocycle shifted upfield due to the encapsulation into the hydrophobic environment.

Highly accurate method for the selective determination of the egression rate constant

When the fluorescence intensity change due to a simple host-guest association is monitored in a stopped-flow measurement, the kinetic traces have three unknown parameters: the rate constants of the formation and disassembly of the 1:1 complex and the ratio of the fluorescence efficiency for the free and bound guests at the monitoring wavelength. These variables can be calculated by least-squares fit of the experimental data but the results usually have considerable uncertainties. To enhance the accuracy of the derived values, we designed experiments whose results can be analysed by two-parameter fitting procedures.

The dissociation rate of Fla–CB7 inclusion complex can be selectively measured by addition of a high affinity binder (A), which rapidly occupies the cavity of practically all free CB7 blocking thereby the back formation of Fla–CB7 and promoting its dissociation.



If A–CB7 has a very large stability constant, its dissociation is negligible on the timescale of the measurement. The concentration of A should be chosen to ensure that $k_+[\text{Fla}] \ll k_A[\text{A}]$. Moreover, A and A–CB7 should not absorb at the excitation wavelength used in the kinetic studies. 1-Adamantylammonium cation meets all of these requirements. Due to its ideal size complementarity and rigidity, it has an extremely large³⁹ ($K_A = 1.7 \times 10^{14} \text{ M}^{-1}$) association constant with CB7. Assuming diffusion controlled complexation, whose rate constant is $k_{\text{diff}} = 6.5 \times 10^9 \text{ M}^{-1} \text{ s}^{-1}$ in water,⁴⁰ $k_{-A} = k_{\text{diff}} / K = 3.8 \times 10^{-5} \text{ s}^{-1}$ is estimated as an upper limit for the rate constant of A egression from CB7 cavity. This corresponds to $t_{1/2} = (\ln 2) / k_{-A} > 5 \text{ h}$ half-life for the first-order dissociation of A–CB7 complex. Therefore, the rate of A exit from CB7 can be neglected on the time-scale of the stopped-flow experiments. The estimated k_{-A} value is close to the rate constant of N-alkyl-1-adamantylammonium egression from CB7 ($(2.4 \pm 0.1) \times 10^{-5} \text{ s}^{-1}$) obtained by Isaacs' group using NMR spectroscopy²³ suggesting that A ingress into CB7 is indeed close to diffusion controlled.

Figure 4A presents the fluorescence intensity change at 440 nm after rapid addition of 3.0 μM A solution to Fla and CB7 mixture at various temperatures. The initial concentrations of the latter two compounds were kept constant (0.15 μM). The dissociation of Fla–CB7 complex is quickly followed by the entry of A in CB7 cavity leading to very stable A–CB7. Consequently, A gradually replaces Fla in CB7 and the stopped-flow signal reflects the diminution of the Fla–CB7 concentration. The fluorescence intensity reaches the level observed for Fla aqueous solution indicating the total removal of Fla from CB7 into water. As Fla egression is a first-order

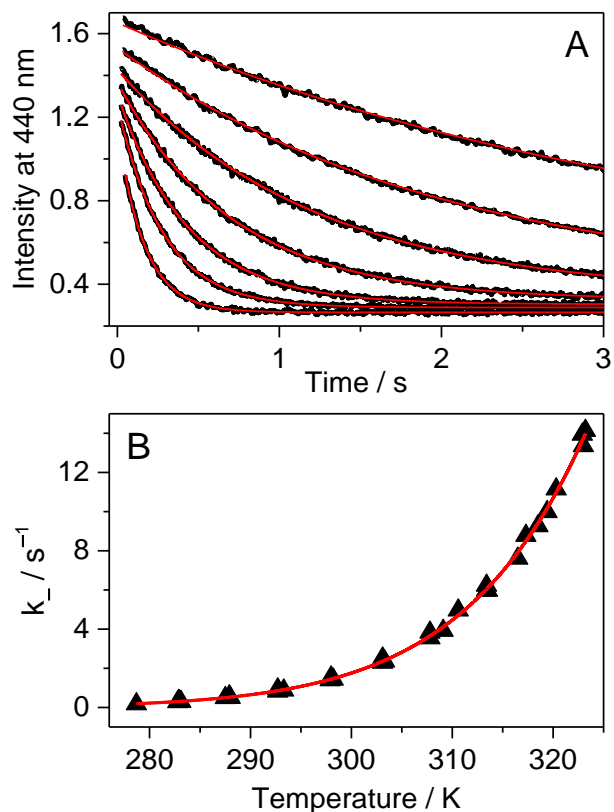


Figure 4 (A) Stopped-flow signals after the addition of 3.0 μM 1-adamantylamine in water to 0.15 μM Fla and 0.15 μM CB7 aqueous solution at 283, 288, 293, 298, 303, 308 and 314 K (from top to down). Excitation and detection were performed at 350 and 440 nm, respectively. (B) Temperature dependence of the rate constant of Fla–CB7 complex dissociation in water. The red lines represent the results of the nonlinear least-squares analysis.

process, its rate constant can be obtained by the nonlinear least-squares fit of an exponential function to the stopped-flow signal.

$$I = I_0 \exp(-k_- t) + I_\infty \quad (3)$$

The method permits straightforward and highly accurate determination of k_- values. For Fla exit from CB7 at 298 K, $k_- = 1.6 \pm 0.2 \text{ s}^{-1}$ is calculated.

To get information on the activation parameters, the experiment was repeated at various temperatures. (Figure 4A) The fluorescence intensities immediately after rapid mixing lessen with the rise of temperature because of two reasons: (i) the fraction of encapsulated Fla becomes smaller due to the diminution of the binding constant and (ii) the fluorescence quantum yield slightly decreases at elevated temperature. The combined effect of these changes causes the diminution of the I_0 and I_∞ parameters in eq 3 with increasing temperature. The initial segment of the stopped-flow signals gradually steepens with rising temperature indicating the acceleration of the exit of Fla from CB7. The analysis of the kinetic results using eq 3 led to the rate constants presented in Figure 4B. The temperature dependence of k_- values was fitted with the Arrhenius equation $k_- = A \exp(-E_a/RT)$, where R denotes the gas constant. The calculated

Table 2 Comparison of the kinetic and thermodynamic parameters for the reversible binding of Fla and berberine in CB7

	Flavopereirine		Berberine ^a	
	Ingression	Egression	Ingression	Egression
k at 298 K	$(9.0 \pm 0.9) \times 10^7$ $M^{-1}s^{-1}$	$1.6 \pm 0.2 s^{-1}$	$(1.9 \pm 0.1) \times 10^7$ $M^{-1}s^{-1}$	$0.81 \pm 0.08 s^{-1}$
A	$(6.1 \pm 3.5) \times 10^{13}$ $M^{-1}s^{-1}$	$(6.3 \pm 2.6) \times 10^{12} s^{-1}$	$(2.0 \pm 1.0) \times 10^{13}$ $M^{-1}s^{-1}$	$(1.8 \pm 1.0) \times 10^{12} s^{-1}$
E_a	33 ± 2 kJ mol ⁻¹	72 ± 2 kJ mol ⁻¹	35 ± 2 kJ mol ⁻¹	71 ± 2 kJ mol ⁻¹
ΔH^\ddagger	31 ± 2 kJ mol ⁻¹	69 ± 2 kJ mol ⁻¹	32 ± 2 kJ mol ⁻¹	69 ± 2 kJ mol ⁻¹
ΔS^\ddagger	11 ± 7 J mol ⁻¹ K ⁻¹	-8 ± 3 J mol ⁻¹ K ⁻¹	2.6 ± 1.9 J mol ⁻¹ K ⁻¹	-19 ± 3 J mol ⁻¹ K ⁻¹
K at 298 K	$(6.1 \pm 0.4) \times 10^7 M^{-1}$		$(2.4 \pm 0.3) \times 10^7 M^{-1}$	
ΔH^b	-37 ± 2 kJ mol ⁻¹		-37 ± 2 kJ mol ⁻¹	
ΔS^b	25 ± 7 J mol ⁻¹ K ⁻¹		17 ± 6 J mol ⁻¹ K ⁻¹	

^a reference 24, ^b derived from the temperature dependence of the binding constant

activation energies (E_a) and A factors are included in Table 2. On the basis of the transition-state theory, the meaning of these parameters can be interpreted by the following relationships:

$$E_a = \Delta H^\ddagger + RT \quad (4)$$

$$A = e \frac{k_B T}{h} \exp\left(\frac{\Delta S^\ddagger}{R}\right) \quad (5)$$

where k_B , h , ΔS^\ddagger , and ΔH^\ddagger denote the Boltzmann and Planck constants, standard entropy and enthalpy of activation, respectively. The ΔS^\ddagger and ΔH^\ddagger quantities derived according to eqs 4 and 5 are also listed in Table 2.

Kinetics of Fla ingress in CB7

The mixing of equimolar Fla and CB7 solutions results in fluorescence intensity enhancement because host-guest binding leads to an almost 4-fold rise in the fluorescence quantum yield of Fla (Table 1). To decelerate the inclusion complex formation, dilute (0.18 μM) reactant solutions were used. Figure 5A presents the normalized fluorescence intensity versus time profiles at various temperatures. Above 304 K, the accuracy of measurements diminishes due to the fast rise of the stopped-flow signals. The experimental data can be described well by assuming simple 1:1 encapsulation equilibrium. In this case, the rates of Fla–CB7 formation and Fla concentration diminution are given as follows:

$$\frac{d[\text{Fla-CB7}]}{dt} = k_+[\text{Fla}][\text{CB7}] - k_-[\text{Fla} - \text{CB7}] \quad (6)$$

$$-\frac{d[\text{Fla}]}{dt} = k_+[\text{Fla}][\text{CB7}] - k_-[\text{Fla} - \text{CB7}] \quad (7)$$

The rate constant of Fla confinement in CB7 (k_+) was calculated by the nonlinear least-squares fit of the numerical solution of eq 6 and 7 to the results of stopped-flow measurements. To

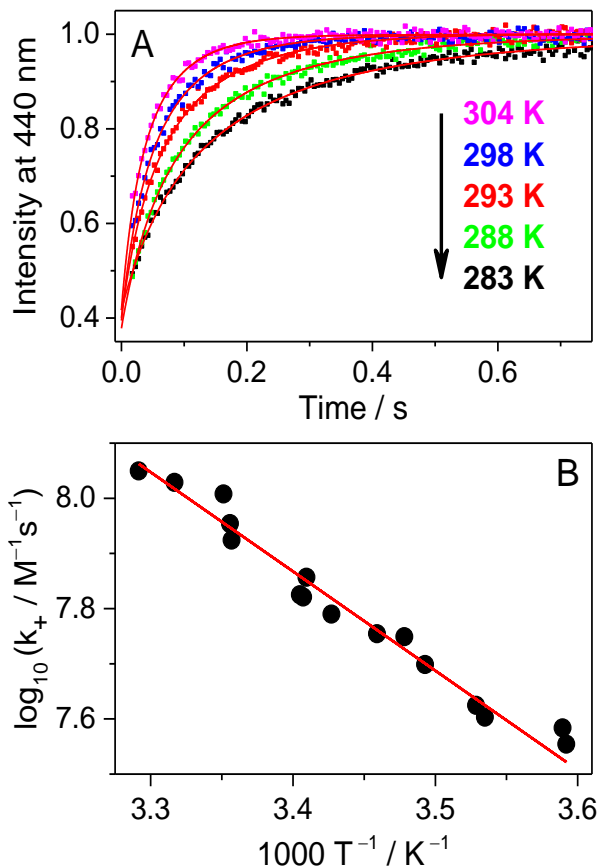


Figure 5 (A) Alteration of stopped-flow results with temperature at 0.18 μM initial Fla and CB7 concentrations in water. Excitation and detection were carried out at 384 and 440 nm, respectively. (B) Arrhenius plot of the rate constant of Fla inclusion in CB7

diminish the uncertainty of k_+ , k_- values determined by independent experiments (vide supra) were kept constant in the regression analysis. Further details of the data analysis are provided in Supplementary Information. The logarithm of the calculated k_+ values is plotted against reciprocal temperature in Figure 5B and the kinetic parameters of host-guest binding are summarized in Table 2. Substantial activation energy is found for the inclusion in CB7, whereas the Arrhenius pre-exponential factor is more than one order of magnitude larger for the association than for the reverse process.

Temperature dependence of the binding constant

The considerable fluorescence intensity enhancement upon Fla confinement in CB7 (Figure 1) was employed to measure the binding constant (K). As a representative example, Figure S2 in Supplementary Information presents the result of fluorescence titration at three temperatures. The analysis of these data led to $K = 7.7 \times 10^6 \text{ M}^{-1}$ for the association constant at 355 K. The significant growth of K with decreasing temperature raised the uncertainty of the determined values around room temperature because increasing segments of the titration curves consisted of two straight lines, which did not contain information about the binding affinity. Therefore, association constants were derived as a ratio of the rate constants of the forward and reverse reactions, $K = k_+/k_-$ below 304 K. Above this temperature the accuracy of k_+ is not high enough to calculate reliable K from kinetic measurements due to the accelerated complex formation and the limited time resolution of the stopped-flow technique, but fluorescence titrations provide

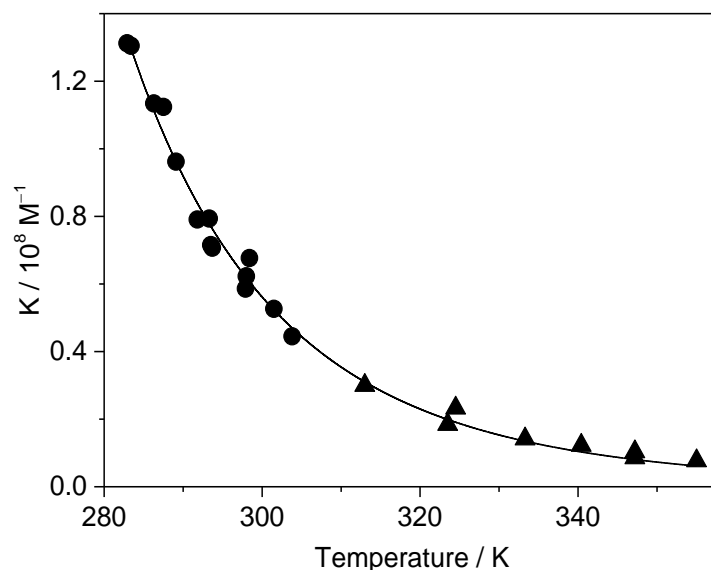


Figure 6 Binding constant of Fla encapsulation in CB7 in water as a function of temperature derived from stopped-flow measurements (●) and fluorescence titrations (▲)

accurate results. Figure 6 demonstrates that the binding constants obtained by stopped-flow and direct fluorescence titration experiments complement each other well. The line represents the result of nonlinear least-squares fit of the relationship

$$K = \exp\left(\frac{\Delta S}{R}\right)\exp\left(-\frac{\Delta H}{RT}\right) \quad (8)$$

The calculated function matches well the experimental data and the acquired enthalpy (ΔH) and entropy (ΔS) changes are incorporated in Table 2.

DISCUSSION

NMR measurements in agreement with quantum chemical calculations showed the partial encapsulation of Fla in CB7. The predominant fraction of the substituted six-membered heterocyclic ring and its ethyl moiety were located inside the cavitand. Hydrophobic interactions and electrostatic attraction with the considerable negative charge density of the portal and the inner surface of the macrocycle⁴¹ promoted the embedment in the apolar core of the host. The considerable fluorescence intensity rise upon confinement and the high fluorescence quantum yield of the inclusion complex allowed the use of very low ($< 0.2 \mu\text{M}$) Fla concentrations in our kinetic studies. This offered several advantages: (i) the bimolecular host-guest binding became slow even in neat water, (ii) the kinetic traces had more than 100 data points permitting accurate determination of the fitted parameters, (iii) addition of competing ions was not needed to monitor the association kinetics in the time range accessible to stopped-flow method, which (iv) simplified the data analysis and allowed determination of activation parameters.

All experimental results could be rationalized by one step binding equilibrium. Intermediate or exclusion complex formation was not observed. Intermediary association complexes were found when cucurbit[6]uril (CB6) served as a host for 4-

methylbenzylammonium,⁴² or cyclohexylmethylammonium^{43,44} as well as for 2-aminoanthracenium confinement in CB7²⁹. The hydrogens of the NH₃⁺ substituent of these guests have considerable partial positive charge, which facilitates electrostatic interaction and hydrogen bonding with the electron-rich oxygens at the rim of CBn cavitands. These effects stabilize the exclusion complex in which the hydrophobic moiety remains in the aqueous phase. Nau and co-workers proposed the transformation of an ammonium type of exclusion complex into the thermodynamically more stable inclusion complex by a “flip-flop” manner.^{43,44} Such a mechanism is not possible for Fla binding because it cannot form hydrogen bond with CB7 and its positive charge is delocalized.

The results summarized in Table 2 demonstrate that Fla has a high binding affinity to CB7. The inclusion is an exothermic enthalpy-controlled process ($\Delta H = -37 \text{ kJ mol}^{-1}$). The entropic term has $-T\Delta S \approx -7.5 \text{ kJ mol}^{-1}$ contribution to the driving force of complexation. The entropy gain arises from the expulsion of water molecules from the cavity of CB7 and from the solvate shell of Fla upon the encapsulation. The entropy loss caused by the host–guest association only partly compensates these effects. The rate constant of ingress of Fla into CB7 is ~70-fold lower ($k_+ = 9.0 \times 10^7 \text{ M}^{-1} \text{ s}^{-1}$ at 298 K) than that of the diffusion-controlled process ($k_{\text{diff}} = 6.5 \times 10^9 \text{ M}^{-1} \text{ s}^{-1}$) in water.⁴⁵ The substantial activation enthalpy (31 kJ mol^{-1}) decelerates the binding process. In addition to the activation enthalpy, the binding enthalpy must be supplied to induce the dissociation of Fla–CB7 complex. Because of the high activation barrier, the exit from CB7 is slow and has a rate constant of 1.6 s^{-1} at 298 K. Our results suggest that the entry into and exit from the relatively rigid CB7 host is sterically hindered.

Activation parameters of the confinement in CB7 were reported only for berberine.²⁴ The activation enthalpies (ΔH^\ddagger) of the ingress and egress agree within the limit of experimental

errors for Fla and berberine (Table 2). This may indicate that an oval distortion of the carbonyl-laced entrance of the CB7 is needed for the penetration of these guests into the interior of the macrocycle as well as for the dissociation of the produced complex. Such a structural change was found to occur when bulky guests were reversibly accommodated in the smaller CB6 cavitand.^{43,44,46,47} The rate constant of the ingress into CB7 is almost 5-fold larger for Fla than for berberine. This difference is primarily attributed to the more favourable activation entropy of Fla–CB7 formation. The ingress of the ethyl moiety of Fla into CB7 probably leads to a looser-bound transition state in which fewer degrees of freedom become limited than in the case of the entry of the dimethoxybenzene moiety of berberine. The positive ΔS^\ddagger of the inclusion complex formation implies that the partial desolvation of the guest and the interior of CB7 more significantly overcompensate the entropy diminution due to the ordering of the reactants into the transition state. The negative ΔS^\ddagger for the egression from CB7 indicates that the delimitation of the degrees of freedom in going to the transition state only partially balances the unfavourable entropy change caused by the coordination of water molecules. Because of the looser-bound structure of the activated complex, the exit of Fla from CB7 has less negative ΔS^\ddagger than the corresponding process of berberine. Therefore, the dissociation rate of Fla–CB7 is a factor of two higher than that of berberine–CB7. The larger stability constant (K) of the former complex originates from the more substantial entropy gain upon Fla encapsulation. Fla fits less tightly in CB7 than berberine. As a consequence, the entropy diminution brought about by the restricted movement of the guest in CB7 offsets the entropy gain due to the release of water molecules upon binding to a lesser extent when Fla is confined instead of berberine. The release of the high-energy water molecules from the apolar core of cucurbiturils is the most important factor determining the stability of the inclusion complexes.^{48,49} No difference was found between the

enthalpies of the CB7 complex formation of Fla and berberine because the desolvation of these hydrophobic compounds has similar and small effect on the exothermicity of the inclusion.

In the case of Fla at 298 K, the rate constant of ingress into CB7 ($k_+ = 9.0 \times 10^7 \text{ M}^{-1} \text{ s}^{-1}$) falls between the values reported for (*R*)-(+)-2-naphthyl-1-ethylammonium²⁶ ($k_+ = 6.3 \times 10^8 \text{ M}^{-1} \text{ s}^{-1}$) and ethyl benzyl ketone⁵⁰ ($k_+ = 4.6 \times 10^6 \text{ M}^{-1} \text{ s}^{-1}$). Despite the 7-fold slower entry of Fla than (*R*)-(+)-2-naphthyl-1-ethylammonium, the binding constant of Fla ($K = 6.1 \times 10^7 \text{ M}^{-1}$ at 298 K) is significantly higher than that of the latter compound²⁶ ($K = 1.1 \times 10^7 \text{ M}^{-1}$) indicating the lack of correlation between the kinetic parameters and the binding affinity. Because of a weaker steric hindrance, the smaller size of (*R*)-(+)-2-naphthyl-1-ethylammonium permits the more rapid egression from CB7 ($k_- = 55 \text{ s}^{-1}$)²⁶ which results in a lower stability of the inclusion complex compared with that of Fla–CB7.

CONCLUSIONS

Fla produces a remarkably stable 1:1 inclusion complex with CB7 in water. Only the ethyl group and the substituted 6-membered nitrogen heterocyclic moiety of the alkaloid are embedded in the hydrophobic core of the host macrocycle. The large equilibrium constant of Fla–CB7 formation is attributed primarily to the considerable enthalpy gain but the entropy growth upon the release of water from the CB7 cavity and the solvate shell of the reactants also has favourable contribution. The complexation is significantly slower than a diffusion-controlled process because Fla cannot freely pass through the portal of CB7. The rate constant of ingress is controlled by steric effects, which depend on the relative size of the guest and the openings of the host macrocycle. In addition to these factors, the enthalpy change of host-guest binding affects the rate of egression from CB7. The entry into this molecular container is expected to occur

without formation of an intermediate if the guest molecule possesses delocalised positive charge and unable to form a hydrogen bond with the carbonyl-lined opening of the host. The fluorescent method based on the competitive binding of 1-adamantylammonium cation to CB7 can be used for the simple, rapid, and highly accurate determination of the egression rate constant also in the case of other guests.

ACKNOWLEDGEMENT

This work was supported by the BIONANO_GINOP-2.3.2-15-2016-00017 project and by the Hungarian Scientific Research Fund (OTKA, Grant K104201). The authors are grateful for the support.

References

- 1 D. H. Macartney, *Isr. J. Chem.*, 2011, **51**, 600-615.
- 2 X. Ma and Y. Zhao, *Chem. Rev.*, 2015, **115**, 7794-7839.
- 3 S. Walker, R. Oun, F. J. McInnes and N. J. Wheate, *Isr. J. Chem.*, 2011, **51**, 616-624.
- 4 K. M. Park, K. Suh, H. Jung, D. W. Lee, Y. Ahn, J. Kim, K. Baek and K. Kim, *Chem. Commun.*, 2009, 71-73.
- 5 I. Ghosh and W. M. Nau, *Adv. Drug Deliv. Rev.*, 2012, **64**, 764-783.
- 6 D. H. Macartney, in *Reference Module in Chemistry, Molecular Sciences and Chemical Engineering*, Elsevier, 2013.
- 7 V. D. Uzunova, C. Cullinane, K. Brix, W. M. Nau and A. I. Day, *Org. Biomol. Chem.*, 2010, **8**, 2037-2042.

- 8 G. Hettiarachchi, D. Nguyen, J. Wu, D. Lucas, D. Ma, L. Isaacs and V. Briken, *Plos One*, 2010, **5**, e10514.
- 9 A. R. Kennedy, A. J. Florence, F. J. McInnes and N. J. Wheate, *Dalton Transactions*, 2009, 7695-7700.
- 10 N. J. Wheate, D. P. Buck, A. I. Day and J. G. Collins, *Dalton Transactions*, 2006, 451-458.
- 11 R. B. Wang and D. H. Macartney, *Org. Biomol. Chem.*, 2008, **6**, 1955-1960.
- 12 I. W. Wyman and D. H. Macartney, *Org. Biomol. Chem.*, 2010, **8**, 247-252.
- 13 N. Saleh, A. L. Koner and W. M. Nau, *Angew. Chem. Int. Ed.*, 2008, **47**, 5398-5401.
- 14 N. Dong, S. F. Xue, Q. J. Zhu, Z. Tao, Y. Zhao and L. X. Yang, *Supramol. Chem.*, 2008, **20**, 659-665.
- 15 R. Wang, I. W. Wyman, S. Wang and D. H. Macartney, *J. Incl. Phenom. Macrocycl. Chem.*, 2009, **64**, 233-237.
- 16 Z. Miskolczy, M. Megyesi, G. Tárkányi, R. Mizsei and L. Biczók, *Org. Biomol. Chem.*, 2011, **9**, 1061-1070.
- 17 M. Megyesi, L. Biczók and I. Jablonkai, *J. Phys. Chem. C*, 2008, **112**, 3410-3416.
- 18 G. Ghale, A. G. Lanctôt, H. T. Kreissl, M. H. Jacob, H. Weingart, M. Winterhalter and W. M. Nau, *Angew. Chem. Int. Ed.*, 2014, **53**, 2762-2765.
- 19 C. F. Li, L. M. Du and H. M. Zhang, *Spectrochim. Acta, Part A*, 2010, **75**, 912-917.
- 20 C. F. Li, L. M. Du, W. Y. Wu and A. Z. Sheng, *Talanta*, 2010, **80**, 1939-1944.
- 21 C. Bohne, *Chem. Soc. Rev.*, 2014, **43**, 4037-4050.
- 22 M. H. Tootoonchi, S. Yi and A. E. Kaifer, *J. Am. Chem. Soc.*, 2013, **135**, 10804-10809.
- 23 P. Mukhopadhyay, P. Y. Zavalij and L. Isaacs, *J. Am. Chem. Soc.*, 2006, **128**, 14093-14102.

- 24 Z. Miskolczy and L. Biczók, *J. Phys. Chem. B*, 2014, **118**, 2499-2505.
- 25 Z. Miskolczy, J. G. Harangozó, L. Biczók, V. Wintgens, C. Lorthioir and C. Amiel, *Photochem. Photobiol. Sci.*, 2014, **13**, 499-508.
- 26 H. Tang, D. Fuentealba, Y. H. Ko, N. Selvapalam, K. Kim and C. Bohne, *J. Am. Chem. Soc.*, 2011, **133**, 20623-20633.
- 27 S. Senler, B. Cheng and A. E. Kaifer, *Org. Lett.*, 2014, **16**, 5834-5837.
- 28 B. Held, H. Tang, P. Natarajan, C. P. da Silva, V. de Oliveira Silva, C. Bohne and F. H. Quina, *Photochem. Photobiol. Sci.*, 2016, **15**, 752-757.
- 29 S. S. Thomas and C. Bohne, *Faraday Discuss.*, 2015, **185**, 381-398.
- 30 N. A. Hughes and H. Rapoport, *J. Am. Chem. Soc.*, 1958, **80**, 1604-1609.
- 31 J. C. P. Steele, N. C. Veitch, G. C. Kite, M. S. J. Simmonds and D. C. Warhurst, *J. Nat. Prod.*, 2002, **65**, 85-88.
- 32 M. Reina, W. Ruiz-Mesia, M. López-Rodríguez, L. Ruiz-Mesia, A. González-Coloma and R. Martínez-Díaz, *J. Nat. Prod.*, 2012, **75**, 928-934.
- 33 Z. Miskolczy, M. Megyesi, L. Biczók and H. Görner, *Photochem. Photobiol. Sci.*, 2011, **10**, 592-600.
- 34 X. Yao, X. Wang, T. Jiang, X. Ma and H. Tian, *Langmuir*, 2015, **31**, 13647-13654.
- 35 M. Megyesi and L. Biczók, *J. Phys. Chem. B*, 2010, **114**, 2814-2819.
- 36 M. Megyesi, L. Biczók and H. Görner, *Photochem. Photobiol. Sci.*, 2009, **8**, 556-561.
- 37 C. Marquez and W. M. Nau, *Angew. Chem. Int. Ed.*, 2001, **40**, 4387-4390.
- 38 Z. Qi and C. A. Schalley, *Acc. Chem. Res.*, 2014, **47**, 2222-2233.
- 39 S. Moghaddam, C. Yang, M. Rekharsky, Y. H. Ko, K. Kim, Y. Inoue and M. K. Gilson, *J. Am. Chem. Soc.*, 2011, **133**, 3570-3581.

- 40 S. L. Murov, I. Carmichael and G. L. Hug, eds., *Handbook of photochemistry*, Marcel Dekker, New York, 1993.
- 41 J. W. Lee, S. Samal, N. Selvapalam, H. J. Kim and K. Kim, *Acc. Chem. Res.*, 2003, **36**, 621-630.
- 42 R. Hoffmann, W. Knoche, C. Fenn and H.-J. Buschmann, *J. Chem. Soc., Faraday Trans.*, 1994, **90**, 1507-1511.
- 43 C. Marquez and W. M. Nau, *Angew. Chem. Int. Ed.*, 2001, **40**, 3155-3160.
- 44 C. Márquez, R. R. Hudgins and W. M. Nau, *J. Am. Chem. Soc.*, 2004, **126**, 5806-5816.
- 45 M. Montalti, A. Credi, L. Prodi and M. T. Gandolfi, *Handbook of Photochemistry; 3rd ed.*, CRC Press: Boca Raton, FL, 2006.
- 46 W.-H. Huang, P. Y. Zavalij and L. Isaacs, *Acta Crystallographica Section E*, 2007, **63**, o1060-o1062.
- 47 W.-H. Huang, P. Y. Zavalij and L. Isaacs, *Acta Crystallographica Section E*, 2008, **64**, o1321-o1322.
- 48 F. Biedermann, V. D. Uzunova, O. A. Scherman, W. M. Nau and A. De Simone, *J. Am. Chem. Soc.*, 2012, **134**, 15318-15323.
- 49 F. Biedermann, M. Vendruscolo, O. A. Scherman, A. De Simone and W. M. Nau, *J. Am. Chem. Soc.*, 2013, **135**, 14879-14888.
- 50 E. Mezzina, F. Cruciani, G. F. Pedulli and M. Lucarini, *Chem. Eur. J.*, 2007, **13**, 7223-7233.